Absorption Coefficients of GaN / Al$_x$Ga$_{1-x}$N Core-Shell Spherical Quantum Dot

D. Abouelaoualim*, A. Elkadadra, A. Oueriagli, A. Outzourhit

LPSCM,Department of Physics, Faculty of Sciences Semlalia,
Cadi Ayaad University P.O. Box 2390, 40000 Marrakech, Morocco

The total absorption coefficient in spherical GaN/Al$_x$Ga$_{1-x}$N core-shell nanodots is theoretically investigated taking into account effective mass approximation. The influence of the nanosystem geometry upon the energy spectrum and transition energy δE associated to interlevel transitions is studied. We found that the energy transitions vary with the core-shell radius, and the peak position of the total absorption coefficient is greatly affected by changing of the shell radius. The possibility of tuning the resonant energies by using the geometric core shell effect of the spatial confinement can be useful in the optoelectronic devices applications. Also we observed that the magnitudes of the total absorption coefficient can be increased significaticaly compared traditional cases of QD, and the peaks are shifted to the lower energies.

Keywords: Quantum dot, Core-shell, Optical absorption.

PACS numbers: 73.21.Ac, 78.67.Pt

1. INTRODUCTION

The interest in the study of the physical properties of confined quantum systems such as quantum wells [1], nanowires [2], and quantum dots (QDs) [3], has increased with the recent progress in semiconductor nanotechnology. In these structures the precise engineering would enable us to confine the charge carriers motion in one, two or three dimensions. Quantum dots can be used to make not just better optical devices [4], but also as optical data storage medium, where bits of information are stored as electrons or holes confined within the dots [5]. One advantage of these is that since the information is typically stored as a single (or few) electron, these devices should require a very low switching energy. The charge to be stored in the dots can be written by optical illumination, which, by wavelength selective writing or local probe techniques, can approach the situation where each quantum dot carries a bit of information. Such quantum dot optical memory devices could potentially achieve ultra-dense storage capacities of Terabit/in2. Recently, in order to aim of improving the electronic structures and optical properties of QDs structure single photon detector for application as an optical data storage medium , different shapes and various confinement potentials have been widely studied, using the effective mass and parabolic one band approximations [6]. In this regard, we consider a GaN/Al$_x$Ga$_{1-x}$N core-shell spherical quantum dot (CSQD)and an interest in the optical phenomena based on intersubband transitions in such structure, the optical. Because the confinement of quasiparticles in such structure leads to the enhancement of the oscillator strength of electron impurity excitations. Meanwhile, the dependence of the optical transition energy on the confinement strength (or dot size) allows the tunability of the resonance frequency. The outline of the paper is as follows: Hamiltonian, the relevant eigenvalues and eigenfunctions of an electron confined in a CSQD are described in Section 2. In Section 3, analytical expressions for the linear and nonlinear intersubband optical ACs and RI changes are obtained using the density matrix approach and the iterative method. Our numerical results and a brief conclusion are presented in Sections 4 and 5, respectively.

2. MODEL AND THEORY

The model used in calculation and analyses is an isolated GaN/Al$_x$Ga$_{1-x}$N core-shell quantum dot with core radius R_1 and shell radius R_2, shown in Fig. 1.
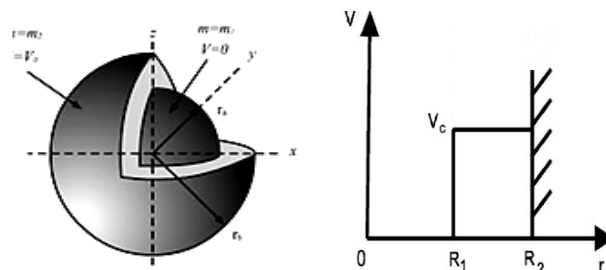
Fig. 1 – Core-shell GaN-Al$_x$Ga$_{1-x}$N quantum dot system showing (a) core and shell layers; and (b) layer potential profile

Suppose the core-shell quantum dot forms a shell well and a centric barrier for the two kinds of materials have different potentials. The potential of the core is chosen to be referent zero point of energy, and the band-gap of GaN is wider than that of Al$_x$Ga$_{1-x}$N, thus VC. On the premise of the effective mass approximation, the steady Schrödinger equation for electron can be written as

$$\left\{-\frac{\hbar^2}{2m_i^* r^2}\left[\frac{\partial}{\partial r}\left(r^2\frac{\partial}{\partial r}\right)+\frac{1}{\sin\theta}\frac{\partial}{\partial\theta}\left(\sin\theta\frac{\partial}{\partial\theta}\right)\right.\right.$$
$$\left.\left.+\frac{1}{\sin^2\theta}\frac{\partial^2}{\partial\varphi^2}\right]+V_i(r)\right\}=E\Phi_{nlm}(r),\qquad(1)$$

where, $\hbar = h/2\pi$, h is Planck's constant; E the energy

* abouelaoualim_d@hotmail.com

eigenvalue; and $\Phi_{nml}(r)$ the responding eigenfunction. n is the principal quantum number, and l and m are the angular momentum quantum numbers. m_i^* is the effective mass of electron in the ith region, $\varepsilon(r)$ constant of core-shell QDs materiels and $V_i(r)$ the potential. They are relative to the position in the model and expressed as follows

$$m_i^* = \begin{cases} m_1^* & r \leq R_1, \\ m_2^* & R_1 < r \leq R_2, \end{cases} \tag{2}$$

$$V_i(r) = \begin{cases} 0, & 0 < r \leq R_1, \\ V_c, & R_1 < r \leq R_2, \\ \infty, & r \rangle R_2, \end{cases} \tag{3}$$

Due to the fact that the mass and the potential are symmetric spherically, the separation of radial and angular coordinates leads to $\Phi_{nml}(r) = R_{nml}(r)Y_{nml}(\theta, \varphi)$, where $R_{nlm}(r)$ is the radial wave function, and $Y_{nlm}(\theta,\varphi)$ is the spherical harmonics n is the principal quantum number, and l and m are the angular momentum quantum numbers. The radial eigenfunction, $R_{nl}(r)$ consists of three parts according to the electron position. Two cases need to be considered for the solution of $R_{nl}(r)$. In regions where electron eigenenergy $E > V_c$, the solution is a linear combination of spherical Bessel function jl and Neumann function nl, written as

$$R_{nl}(r) = \begin{cases} A_1 J_l(k_{nl,1}r) + B_1 n_l(k_{nl,1}r), & r \leq R_1, \\ A_2 J_l(k_{nl,2}r) + B_2 n_l(k_{nl,2}r), & R_1 \langle r \leq R_2, \\ 0, & r \rangle R_2, \end{cases} \tag{4}$$

with

$$k_{nl,1} = \sqrt{2m_1^* E/\hbar^2}, \tag{5}$$

$$k_{nl,1} = \sqrt{2m_2^*(E - V_c)/\hbar^2}, \tag{6}$$

A_1, A_2, B_1 and B_2 are normalized constants. In regions where $E \langle V_c$, the radial wave function is

$$R_{nl}(r) = \begin{cases} A_1' J_l(k_{nl,1}r) + B_1' J_l(k_{nl,1}r), & r \leq R_1, \\ A_2' h_l^{(+)}(k_{nl,2}r), & R_1 \langle r \leq R_2, \\ 0, & r \rangle R_2, \end{cases} \tag{7}$$

with

$$k_{nl,2} = \sqrt{2m_2^*(V_c - E)/\hbar^2}, \tag{8}$$

A_1', A_2' and B_1' are normalized constants.

Let us consider that the system is excited by a monochromatic electromagnetic field, $E(t) = Ee^{i\omega t} + c.c.$, which is polarized along the Z-direction. Therefore, the time evolution of the density operator of the system is given by [7]

$$\frac{\partial \rho}{\partial t} = \frac{1}{i\hbar}\left[H - ME(t), \rho\right] - \Gamma\left(\rho - \rho^0\right), \tag{9}$$

where H is the Hamiltonian of the system in the absence of the electromagnetic field, $M = ez$ is the dipole operator along the Z-axis, ρ^0 is the unperturbed density operator and Γ is the damping operator due to the electron-phonon interaction and the other collision processes. The above equation can be solved using the perturbation method by expanding ρ as [8]

$$\rho = \sum_n \rho^{(n)}, \tag{10}$$

with

$$\frac{\partial \rho_{ij}^{(n+1)}}{\partial t} = \frac{1}{i\hbar}\left\{\left[H, \rho^{(n+1)}\right]_{ij} - \left[M, \rho^{(n)}\right]_{ij} E(t)\right.$$
$$\left. - i\hbar\Gamma_{ij}\partial\rho_{ij}^{(n+1)}\right\}, \tag{11}$$

On the other hand, the electric polarization of the system can be written as

$$P(t) = \varepsilon_0\chi(\omega)Ee^{-i\omega t} + \varepsilon_0\chi(-\omega)Ee^{i\omega t}$$
$$= \frac{1}{V}trace(\rho M), \tag{12}$$

where V is the volume of the system, ε_0 is the permittivity of free space, and trace means the summation over the diagonal elements of the matrix. Using the same density matrix formalism, the analytic expressions of the linear and the third order nonlinear susceptibilities for a two-level quantum system are given and ε' is the real part of the permittivity [9]:

$$\varepsilon_0\chi^{(1)}(\omega) = \frac{\sigma_v |M_{ij}|^2}{E_{ij} - \hbar\omega - i\hbar\Gamma_{ij}}, \tag{13}$$

$$\varepsilon_0\chi^{(3)}(\omega) = \frac{\sigma_v |M_{ij}|^2 |E|^2}{E_{ij} - \hbar\omega - i\hbar\Gamma_{ij}}\left[\frac{4|M_{ij}|^2}{(E_{ij} - \hbar\omega)^2 + (\hbar\Gamma_{ij})^2}\right.$$
$$\left. - \frac{(M_{ff} - M_{jj})^2}{(E_{fj} - i\hbar\Gamma_{if})(E_{fj} - \hbar\omega - i\hbar\Gamma_{if})}\right., \tag{14}$$

where σ_v is the carrier density, $E_{fj} = E_f - E_i$ is the energy interval of the two level system. M_{fj} is the dipole matrix element, which is defined by $M_{fi} = |\langle \Psi_f | er | \Psi_i \rangle|$, $(f, i = 1, 2)$ and Γ shows the damping due to electron-phonon interaction. The absorption coefficient is given by

$$\alpha(\omega) = \omega\sqrt{\frac{\mu}{\varepsilon'}}\,Im(\varepsilon_0\chi(\omega)) \tag{15}$$

The total absorption coefficient $\alpha(\omega, I)$ can be writ-

ten as

$$\alpha(\omega, I) = \alpha^{(1)}(\omega, I) + \alpha^{(3)}(\omega, I) \qquad (16)$$

where I is the incident optical intensity and is defined as

$$I = 2\sqrt{\frac{\varepsilon'}{\mu}}\left|E(\omega)\right|^2 \qquad (17)$$

Here μ is the permeability of the system, and ε' is the real part of the permittivity.

3. NUMERICAL RESULTS AND ANALYSIS

In the numerical calculations carried out for a core-shell quantum dot, the following parameter values have been used [13]: characterize the electrical and optical properties of the physical parameters used in our numerical work for GaN and Al$_x$Ga$_{1 – x}$N are taken from ref [10].The effective mass is $m^*_{GaN} = 0.19m_e$ for GaN $m^*_{Al_xGa_{1-x}N} = (0.19(1-x) + 0.33)m_0$ for Al$_x$Ga$_{1 – x}$N. The real part of permittivity is chosen to be ε. The band-gap is $\Delta E_c = x6.13\ eV + (1-x)3.42\ eV - x(1-x)1.0\ eV$. The conduction band offset is chosen as $V_b = 0.75(E_g(x) - E_g(0))$. The dephasing constant corresponding to elastic scattering is $\Gamma_{13} = 0.14ps$ and the incident optical intensity is $I = 1MW/cm^3$.

By virtue of the importance of intersubband transition, we have studied the variation of energy difference between the ground state to the exited state as a function of CSQDs size, with a GaN core and a Al$_{1 – x}$ Ga$_x$N shell, both of which were assumed to have a wurtzite structure. Such dots have a potential barrier of $V_C = 2.77\ eV$ for both electrons and holes to tunnel through in order to reach the shell from the core. A summary of these calculations is shown in Fig. 2(a), (b). In these graphs, when holding the shell thickness fixed, the energy levels behave similarly to those of QDs, Fig. 2(a). With the core radius fixed, increasing the shell size produces an entirely different trend-both the states Fig. 2(b), move down in energy. This causes the transition energy between those states to be roughly constant. These results imply a simple rule of thumb for this system- the transition energies are primarily determined by the shell radius. In Fig. 3, we display the total AC as function of pump photon energy $\hbar\omega$ for different core radius with a fixed shell radius when the transition energy levels selected in the region where $E < V_c$, namely inside the core well. It is seen from this figure that for the GaN / Al$_{1 – x}$ GaXN core-shell QDs the resonant magnitudes are 6.5×10^7 /m for $R_1 = 42$ Å, Fig. 3(a) . It can be seen that each curve has only one peak which is due to single photon resonance. Furthermore we can find that the total AC increase and the peak shift to lower energy. And the larger the R_1 is, the smaller the peak shift is.

These conclusions regarding the AC spectrum can be physically explained as follows: as a consequence of the quantum size effect, energy distances between


a

b
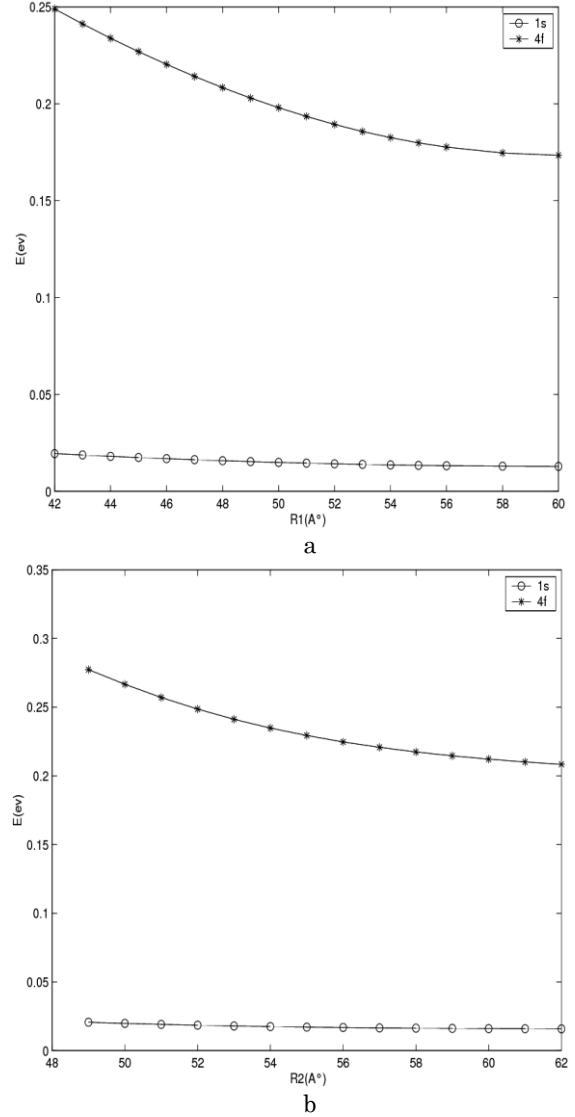
Fig. 2 – Energy levels of GaN / Al$_x$Ga$_{1 – x}$N core-shell quantum dot with (a) fixed shell radius and (b) fixed core radius

electronic states in the conduction band become smaller when R_1 increases, Fig. 2(a), the larger the size is, the smaller the energy distance is; the increase of the dipole matrix element becomes stronger with the increase of the radius. When R_2 increases from 42 Å to 52 Å with a fixed R_1, the peak shift amount to 7×10^7 /m, Fig. 3(b). The reason for this phenomenon is related to electron confinement. When the electron eigenenergy $E < V_C$, electrons are completely confined in the core well and there is nearly no electron distributing in the shell barrier, the probability distribution for the electronic wave function mainly concentrates in the core well. Even though shell layer widens much, contributes a little to electronic wave function and the peak shift as long as the size of core layer keeps a constant.

Effect of barrier mole fraction (as a parameter) on the total AC of the system is illustrated in Fig. 4. We plot the total optical AC as functions of the photon energy and x, with $I = 1MW/cm^2$, $R_1 = 50°$Å and $R_2 = 62$ Å. It is shown that with increase of mole fraction, the absorption peak decreases. This is related to the fact that

a

b
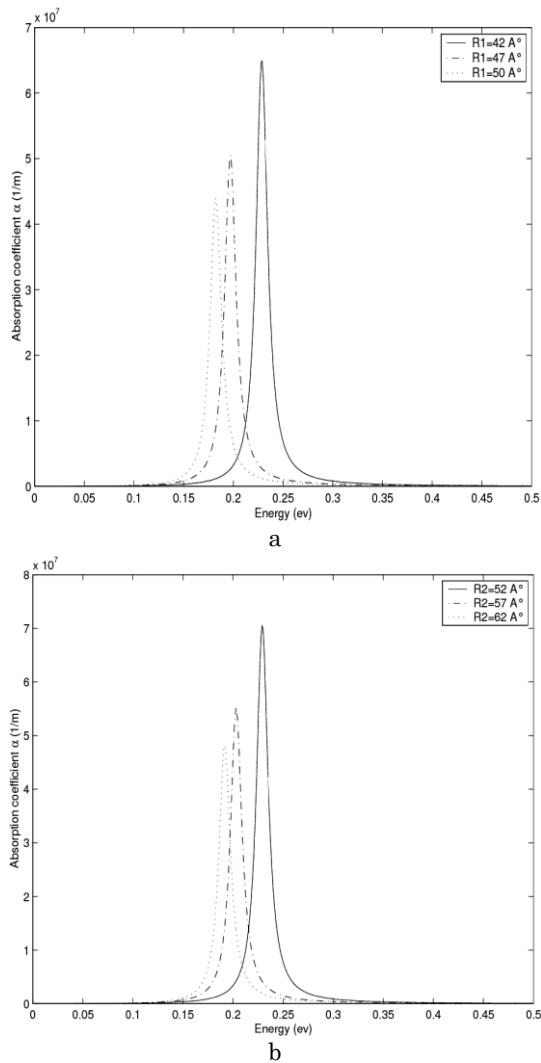
Fig. 3 – Total AC is plotted as functions of the photon energy and (a) core radius R_1 with $R_2 = 62$ Å (b) shell radius R_2 with, $R_1 = 48$ Å; with $I = 1MW/cm^2$ and $x = 0.15$, when $E < V_c$
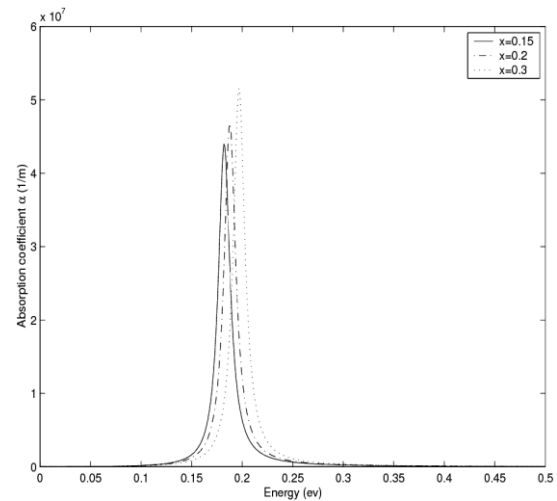
Fig. 4 – Total optical AC as functions of the photon energy and Aluminium concentration x, with $I = 1MW/cm^2$ and $R_1 = 48$ Å and $R_2 = 62$ Å

the transition energy δE. When Aluminum concentration increase, the barrier increases, this enhances the confinement of electrons. As a result, the overlap between electron wave function at two subbands increases, and thus the optical intersubband transition also enhances its intensity.

4. CONCLUSIONS

The total absorption coefficient (AC) of GaN / Al$_x$Ga$_{1-x}$N core-shell spherical quantum dot have been investigated, using the compact-density matrix formalism and an iterative method. We have found that the size double-layered spherical quantum dot parameter has a significantly influence on the total optical AC, and the peaks shift, crease and toward the lower energies as R_1 (R_2) decreases. Also, the Aluminum concentration (the potential height) has significant effects on the optical AC. We expect that this work will be of great help for describing the correct behavior of optical properties in DSQD with different size, which may be useful in technological applications as quantum cryptography or quantum information processing using single photon detector.

REFERENCES

1. H. Carrere, V.G. Truong, X. Marie, R. Brenot, G.de Valicourt, F. Lelarge, T. Amand, *Appl. Phys. Lett.* **97**, 121101 (2010).
2. Hassan H. Hassan, Harold N. Spector, *Phys. Rev. B* **33**, 5456 (1986).
3. D. Abouelaoualim, *Acta Phys. Pol. A* **112**, 49 (2007).
4. Mohammadreza Khorasaninejad, Simarjeet Singh Saini, *Opt. Express* **18**, 23442 (2010).
5. M.R.K. Vahdani, G. Rezaei, *Phys. Lett. A* **373**, 3079 (2009).
6. D. O'Brien, S.P. Hegarty, G. Huyet, A.V. Uskov, *Opt. Lett.* **29**, 1072 (2004).
7. J.C. Blakesley, P. See, A.J. Shields, B.E. Kardynał, P. Atkinson, I. Farrer, D.A. Ritchie, *Phys. Rev. Lett.* **94**, 067401 (2005).
8. H.W. Li, B.E. Kardynał, P. See, A.J. Shields, P. Simmonds, H.E. Beere, D. Ritchie, *Appl. Phys. Lett.* **91**, 073516 (2007).
9. V. Nikolaev, E.A. Avrutin, *Phys. Rev. B* **70**, 125319 (2004).
10. G. Alvarez, Luis G. G. V. Dias da Silva, E. Ponce, E. Dagotto, *Phys. Rev. E* 84, 056706 (2011).
11. Anders M.N. Niklasson, Matt Challacombe, *Phys. Rev. Lett.* **92**, 193001 (2003).
12. T. Takagahara, *Phys. Rev. B* **36**, 9293 (1987).
13. Yen-Kuang Kuo, Wen-Wei Lin, *Jpn. J. Appl. Phys.* **41**, 73 (2002).